Oriented Display of Cello-Oligosaccharides for Pull-down Binding Assays to Distinguish Binding Preferences of Glycan Binding Proteins

Markus Hackla, Zachary Powera, Shishir P. S. Chundawata,*

^a Department of Chemical and Biochemical Engineering, Rutgers, The State University of New Jersey, Piscataway NJ, 08854

*Corresponding author: Shishir P. S. Chundawat (ORCID: 0000-0003-3677-6735). Department of Chemical & Biochemical Engineering, Rutgers, The State University of New Jersey, 98 Brett Road Piscataway, NJ 08854. Phone: +1-848-445-3678

Email: shishir.chundawat@rutgers.edu

Abstract: The production of biofuels from lignocellulosic biomass using carbohydrateactive enzymes like cellulases is key to a sustainable energy production. Understanding the adsorption mechanism of cellulases and associated binding domain proteins down to the molecular level details will help in the rational design of improved cellulases. In nature, carbohydrate-binding modules (CBMs) from families 17 and 28 often appear in tandem appended to the C-terminus of several endocellulases. Both CBMs are known to bind to the amorphous regions of cellulose non-competitively and show similar binding affinity towards soluble cello-oligosaccharides. Based on the available crystal structures, these CBMs may display a uni-directional binding preference towards cello-oligosaccharides (based on how the oligosaccharide was bound within the CBM binding cleft). However, molecular dynamics (MD) simulations have indicated no such clear preference. Considering that most soluble oligosaccharides are not always an ideal substrate surrogate to study the binding of CBMs to the native cell wall or cell surface displayed glycans, it is critical to use alternative reagents or substrates. To better understand the binding of type B CBMs towards smaller cello-oligosaccharides, we have developed a simple solid-state depletion or pull-down binding assay. Here, we specifically orient azidolabeled carbohydrates from the reducing end to alkyne-labeled micron-sized bead surfaces, using click chemistry, to mimic insoluble cell wall surface-displayed glycans. Our results reveal that both family 17 and 28 CBMs displayed a similar binding affinity towards cellohexaose-modified beads, but not cellopentaose-modified beads, which helps rationalize previously reported crystal structure and MD data. This may indicate a preferred uni-directional binding of specific CBMs and could explain their co-evolution as tandem constructs appended to endocellulases to increase amorphous cellulose substrate targeting efficiency. Overall, our proposed workflow can be easily translated to measure the affinity of glycan-binding proteins to click-chemistry based immobilized surface-displayed carbohydrates or antigens.

Keywords: Azido Sugars, Carbohydrate-binding modules (CBMs), Carbohydrate-active enzymes (CAZymes), Click chemistry, Cello-oligosaccharides, Solid-depletion binding assay

1 Introduction

The cost-effective breakdown of lignocellulose biomass waste to fermentable sugars and its subsequent fermentation to ethanol is a crucial process for the production of sustainable fuel in the future (1). In this process, enzymatic hydrolysis of lignocellulosic biomass is an important step and relies on the effective deployment of a mixture of enzymes to hydrolyze the biomass-derived polysaccharides into fermentable sugars (2). Many of those carbohydrate-active enzymes (CAZymes) are multi-domain polypeptides where a single or multiple CBMs are attached to one or more catalytic domains (CDs). The CBM is responsible for the recognition of and binding to the substrate, whereas the CD breaks down the substrate into shorter oligosaccharides or fermentable monosaccharides for direct cellular uptake (3). The CBM, therefore, plays a pivotal role in the depolymerization process since it is often the main driver for substrate recognition and targeting specific regions of the cell wall polysaccharides like cellulose (4, 5). Based on specific substrate affinity, CBMs can be categorized into three groups. Type A CBMs bind to crystalline regions of cellulose, whereas type B and type C CBMs bind to oligosaccharide chains or single monosaccharide units, respectively (6).

The binding sites of type B CBMs range from a deep binding groove, as seen in CBM4 (7-10), to a relatively shallow groove as seen in CBM families 17 and 28 (11-13). Type-B CBMs like CBM 17 and 28 can accommodate between 3 and 6 glucopyranose units of a cello-oligosaccharide within the binding cleft. While type B CBMs exhibit a stronger affinity for insoluble amorphous cellulose compared to Avicel® or microcrystalline cellulose (9, 14–17), these CBMs are also reported to bind short cello-oligosaccharides (9, 11, 14, 16, 18–20). However, the CBM-glycan binding affinity drops with decreasing chain length of the cello-oligosaccharide. Crystal structures of CBMs from families 17 and 28 containing a bound ligand show that the cello-oligosaccharide is actually bound in the opposite direction for each as shown in Figure 1, although the binding free energies as estimated experimentally were similar for both protein families for the same cellooligosaccharide (11-13). MD simulations have been carried out to investigate whether there is any preference for the direction of the ligand docked in the type-B CBM binding pocket (10, 21, 22). The MD study for CBM 17 and 28 (21) revealed that while the cellopentaose ligand was in contact with the CBM over the entire MD simulation period for any orientation of the ligand, not all orientations exhibited equally well-stabilized protein-ligand interactions. In fact, the root mean square fluctuations (RMSF) were around 1 Å for CBM17 binding the ligand from the reducing end and CBM28 binding from the non-reducing end of cellopentaose. The opposite binding orientations (i.e. CBM17 binding from the non-reducing end) showed more than twice as much RMSF as well as sliding of the cellopentaose in the binding pocket, indicating less stable and potentially weaker binding interactions (21).

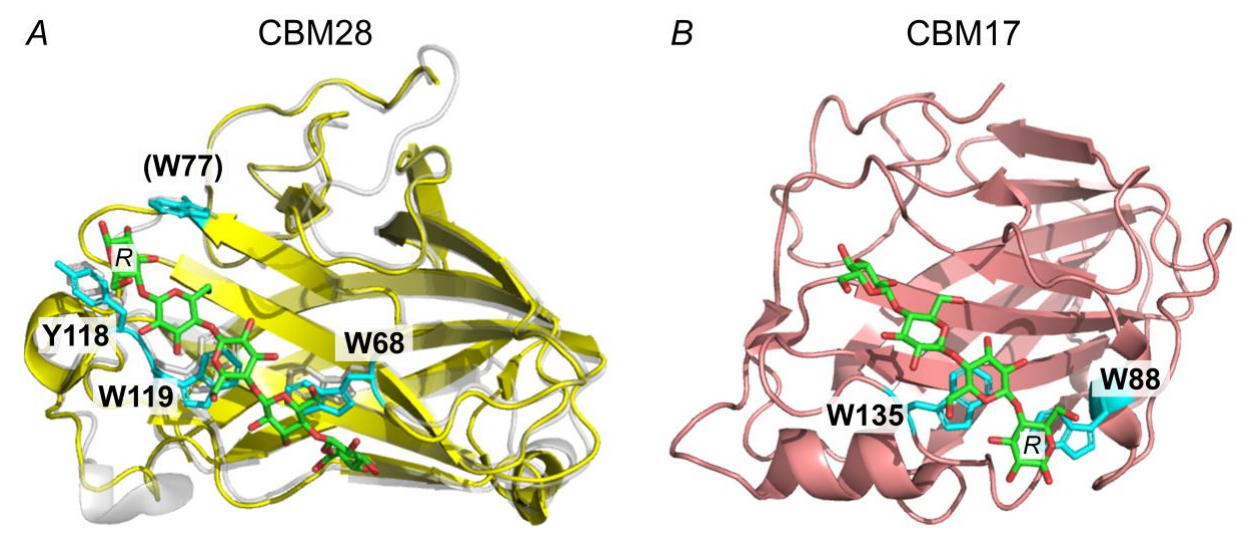


Figure 1: Orientation of cello-oligosaccharides in the binding pocket of type B CBMs. The reducing end of the oligosaccharide is labeled "R" and aromatic residues of the protein in close contact with the oligosaccharide are highlighted in cyan. The cello oligomers are oriented in different directions in the binding pockets. A) No crystal structure of A. akibai CBM28 bound to a ligand exists, hence CBM28 bound to cellopentaose from R. josui (PDB ID 3aci, light grey) was aligned with A. akibai CBM28 (PDB ID 1uww, yellow). Based on structural similarities, potential residues of A. akibai CBM28 are noted. W77 may not be involved in ligand binding with this alignment but may aid in an alternative binding orientation (13). B) CBM17 from C. cellulovarans bound to cellotetraose (PDB ID 1j84).

Bacterial cellulases such as Cel5A from Alkalihalobacillus akibai (formerly known as Bacillus sp. 1139) (18), Cel5A from Ruminoclostridium josui (14), and Cel9B from Cellulomonas fimi (23) contain type B CBMs in tandem. A. akibai and R. josui native tandem design consists of CBM17/CBM28, whereas C. fimi tandem design is constructed of two CBM4. It is hypothesized, that multiple type B CBMs in tandem can help bind different regions of the insoluble and highly disordered cell wall substrate (15). Amorphous regions of cellulose are characterized by a reduced crystallinity and degree of polymerization, although structural details remain obscured (24). It was shown that different type B CBMs bind to different regions of cellulose and cell walls noncompetitively, indicative of recognizing different binding sites on the substrate (25–27). Though, the identification of those different binding sites is difficult to achieve due to the complex nature of the insoluble substrate. Using well-defined substrates, such as cellooligosaccharides, the binding affinity of CBMs can be accurately determined with isothermal titration calorimetry (ITC), fluorescence or ultraviolet (UV) absorption (11, 14, 16, 18–20). However, it is not possible to infer information about the binding configuration of the soluble oligosaccharide ligand in the CBM binding pocket, and the only structural information about ligand orientation stems indirectly from examining crystal structures of CBMs with a bound ligand.

To better understand how type B CBMs bind to solid cellulosic substrates, we developed a well-defined 'amorphous' cellulosic substrate surrogate to perform solid-state depletion assays. Micron-sized polystyrene (PS) beads were functionalized with cello-oligosaccharides that were oriented with a defined stereochemistry (i.e., with the non-reducing end exposed and available for interaction with the solvent). Previous studies have explored the immobilization of carbohydrates on diverse substrates such as nanoparticles, microns-sized beads, or microplates, primarily to enhance the

biocompatibility, biodegradability, and functionality of the nanoparticles for drug delivery. These methods include a broad range of carbohydrates, from simple sugars such as mannose or galactose, to more complex carbohydrates such as hyaluronic acid and employ various immobilized strategies (28–31). Larger carbohydrates, such as pullulan (32), or hyaluronan (33), when immobilized randomly on surfaces, have been shown to alter protein and cell adhesion. Methods such as ITC (34), surface plasmon resonance (SPR) (35) or quartz crystal microbalance (QCM) (36) have been used to study the binding affinity of carbohydrate binding proteins (lectins) to nanoparticles functionalized with small carbohydrates, however, the ligands were not treated as solid substrates.

To our knowledge, the method presented here is the first solid-state depletion assay, in which soluble cello-oligosaccharides with a degree of polymerization (dp) >4 were used to functionalize micron-sized particles and the cello-oligosaccharide is oriented in a defined stereochemistry. An overview of the PS-bead preparation scheme is outlined in Figure 2. Briefly, we use Shoda's reagent (37) to convert cello-oligosaccharides into corresponding glycosyl azides (Figure 2-A). A comprehensive overview of alternative carbohydrate modification methods is found elsewhere (38). Micron-sized PS beads were functionalized with dibenzocyclooctyne (DBCO) (Figure 2-B) and the glycosyl azides were covalently linked to these beads using click-chemistry, creating a proxy insoluble cellulosic substrate with defined properties.

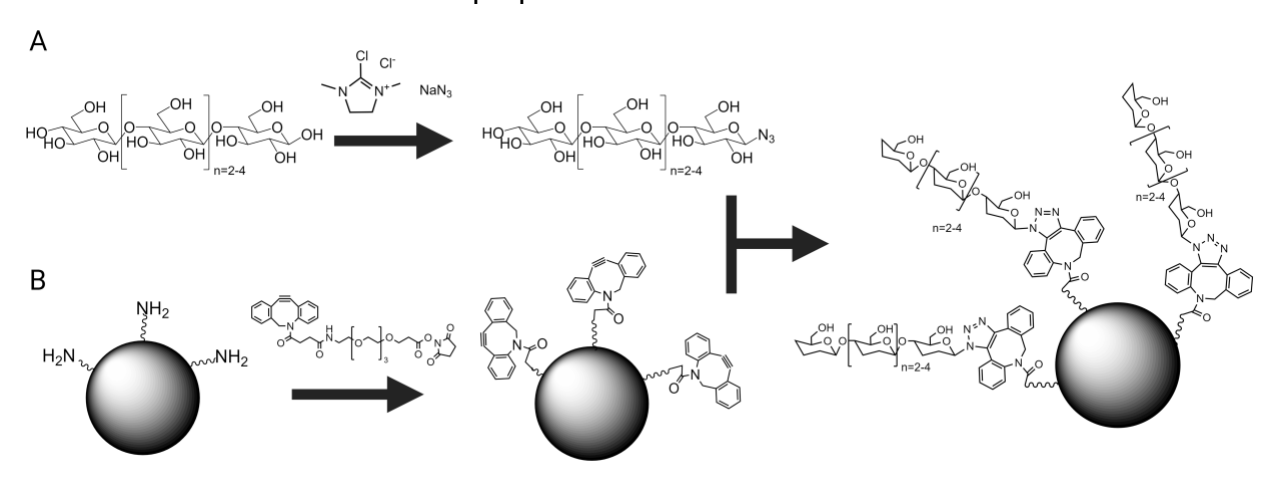


Figure 2: Overview of the method to immobilize soluble cello-oligosaccharides on PS beads using click chemistry to create defined solid substrates. A) The conversion of cello-oligosaccharides to corresponding glycosyl azides using Shoda's reagent (DMC or 2-chloro-1,3-dimethylimidazolinium chloride) and sodium azide. B) Conversion of amino groups displayed on micron-sized PS beads to DBCO groups using a PEGylated NHS-ester. The glycosyl azides are then reacted with the DBCO to create cello-oligosaccharide-modified PS beads as the final product.

The cello-oligosaccharide functionalized PS beads were then used in a solid-state depletion assay to determine the binding properties of CBM28 from *A. akibai* and CBM17 from *C. cellulovarans*. Both CBMs were fused to a green fluorescent protein (GFP) tag for protein quantification. Our results show that the equilibrium binding affinity between CBM17 and CBM28 and cellohexaose-modified beads is comparable. However, there is a difference in binding affinity for cellopentaose-modified beads, which contrasts previous studies where the substrate was free in solution (14). Our method can be applied to immobilize any soluble carbohydrates or oligosaccharides via the reducing end, thus creating an insoluble substrate analog to investigate protein binding at interfaces through

easy-to-execute pull-down assays. More advanced characterization methods such as QCM or SPR can utilize the same workflow, once the QCM/SPR surface is functionalized with DBCO or alkyne moieties for the azide-alkyne cycloaddition, thus highlighting the versatility of the described workflow.

2 Material and Methods

Unless otherwise mentioned, all reagents were either purchased from VWR International, USA, Fisher Scientific, USA, or Sigma-Aldrich, USA. Cello-oligosaccharides were either purchased from Biosynth Carbosynth, USA or Neogen, USA. Amino-modified polystyrene beads (AP-30-10) with a nominal diameter of 3.4 μm were purchased from Spherotech Inc, USA.

2.1 Protein production and purification

The genes for *Clostridium cellulovarans* CBM17 and *Alkalihalobacillus akibai* CBM28, codon optimized for *E.coli*, were obtained from Genewiz, USA, and expressed and purified as GFP-fusion constructs (see Supplemental Figure S1 and Supplemental Table S1) in *E. coli* BL21- CodonPlus(DE3)-RIPL (Stratagene, USA) as described previously (39). Briefly, a 10 ml overnight culture was grown in LB media containing 34 μ g/ml chloramphenicol and 50 μ g/ml kanamycin at 37°C. This overnight culture was used to inoculate 200 ml LB media containing the same antibiotics. The cells were grown at 37°C and 200 rpm until the optical density (OD600) reached 0.4-0.6, after which the expression was induced by adding isopropyl β -D-1-thiogalactopyranoside (IPTG) to a final concentration of 1 mM. The temperature was reduced to 18-25°C and the cells further incubated for 18-24 hours and harvested by centrifugation at 6,000 x g for 15 minutes.

The cell pellets were resuspended in 15 ml of lysis buffer (20 mM sodium phosphate, 500mM NaCl, 20% v/v glycerol, pH 7.4) and lysed by sonication. Next, the cell debris were separated from the supernatant containing the His-tagged GFP-CBMs by centrifugation at 10,000 x g for 40 minutes at 4°C. The supernatant was mixed with 4 ml of nickel- nitrilotriacetic acid (Ni-NTA) functionalized magnetic beads and incubated for 60 minutes at 4°C with constant shaking. The supernatant was removed, and the resin was washed twice with 10 ml IMAC-A buffer (100 mM 3-(N-morpholino) propanesulfonic acid (MOPS), 10 mM imidazole, 500 mM sodium chloride at pH 7.4) and twice with 10 ml buffer containing 95% IMAC-A and 5% IMAC-B (100 mM MOPS, 500 mM imidazole and 500 mM sodium chloride at pH 7.4). Finally, the GFP-CBM constructs were eluted from the resin by incubation in 1 ml IMAC-B for 15 minutes at 4°C. The protein concentration was determined by measuring the absorbance at 280 nm using the molecular weight and molar extinction coefficient of 52.93 kDa, 53,985 M⁻¹cm⁻¹ and 55.47 kDa, 66,935 M⁻¹cm⁻¹ for GFP-CBM17 and GFP-CBM28, respectively. Purity of >90% was confirmed by SDS-PAGE.

2.2 Azide modification of cello-oligosaccharides

The anomeric hydroxy group of the cello-oligosaccharide was substituted with an azide group following the steps outlined by Tanaka et al (40). The reaction mixture composition per 10 mg of the substrate is summarized in Table 1. First, the cello-oligosaccharide was dissolved in the respective amount of heavy water (D₂O) and transferred to a 20 ml screw-

capped glass vial containing a small magnetic stir bar. Next, sodium azide (NaN₃) and 2-chloro-1,3-dimethylimidazolinium chloride (DMC) were added, followed by the addition of N,N-diisopropylethylamine (DIPEA). The reaction mixture was stirred for 30 minutes at room temperature and quenched with twice the reaction mixture volume of deionized (DI) water. Immediately after quenching, the mixture was transferred to a dialysis membrane (SpectrumTM 131060, MWCO 100-500 Da) and dialyzed at room temperature against DI water for 90-170 hours (4-7 days) with replacement of water every 8-24 hours (41). To prevent microbial growth, ProClinTM 300 at 0.05% (v/v) was added between hours 36-84. The final dialysis step (last 8-12 hours) did not contain any additives. After dialysis, the liquid was transferred to a 50 ml conical flask and the water evaporated *in vacuo*. Finally, the solid residue was dissolved in 1 ml of DI water.

Table 1: Reaction mixture composition per 10 mg of cello-oligosaccharide to generate glycosyl azides

	D-Cellotetraose	D-Cellopentaose	D-Cellohexaose
D ₂ O (ml)	0.5	1.0	2.0
NaN₃ (mg)	81.3	162.6	325.2
DMC (mg)	10.6	21.2	42.4
DIPEA (ml)	0.065	0.066	0.132

The conversion and overall yield were quantified through densitometric analysis of thin-layer chromatography (TLC) images. Aluminum-backed TLC silica gel 60 F₂₅₄ plates (Supelco® 1.05554.0001) were spotted with the dialyzed, resuspended reaction mixture and unmodified cello-oligosaccharide control and developed using a mobile solvent mixture of butanol-ethanol-water in a volumetric ratio of 5-5-4 (42). After TLC, the dried plates were sprayed with 0.1% orcinol (in 1.8 M sulfuric acid in 190 proof ethanol), dried, and developed at 100°C for 3-5 minutes until the cello-oligosaccharide spots turned dark. The conversion was calculated as $X = \frac{I_{N3}*A_{N3}}{I_{N3}*A_{N3}+I_{G}*A_{G}}$ where I_{N3} is the pixel intensity of the azide-modified cello-oligosaccharide (glycosyl azide), measured over the spot size A_{N3} . I_{G} and A_{G} represent the mean intensity and spot size of the unmodified cello-oligosaccharide. The concentration was determined by creating a standard curve of the unmodified cello-oligosaccharide at concentrations between 1 mM to 0.1 mM and comparing the intensity of the reaction mixture to the standard curve. The overall yield was calculated as $Y = \frac{n_{N3}}{n_{G}}$, where n_{N3} is the final amount of glycosyl azide and n_{G} is the initial amount of substrate (unmodified cello-oligosaccharide) added.

2.3 Cello-oligosaccharide functionalization of amino-modified PS beads

The steps outlined here describe the preparation of one sample (one data point) for the solid-state depletion assay and scale-up depends on the number of samples required. The control samples for non-specific binding receive the same treatment, except during the click-reaction step, phosphate buffered saline (PBS) was used instead of glycosyl azides. It is important to ensure that all buffers during the functionalization steps are free of azides as it competes with the click reaction of glycosyl azides. The glycosyl azides are covalently linked to the amino-functionalized beads in a two-step process as shown in Figure 2. In the first step, the amino groups on the PS bead surface were converted into DBCO groups. First, 20 µl of bead stock solution (concentration of NH₂ groups is

approximately 250 μ M as per the manufacturer's specification) were spun down and resuspended in PBS at pH 7.4. To functionalize the beads with DBCO, a PEGylated NHS-ester linker was used (i.e., DBCO-polyethylene glycol (PEG(4)) N-hydroxysuccinimidyl (NHS) ester). The beads were resuspended in 20 μ l of 250 μ M DBCO-PEG(4)-NHS ester (linker) in PBS and incubated on a rotisserie overnight at room temperature. The conversion to DBCO moieties was confirmed by analyzing the fluorescence intensity of single beads functionalized with azide-labeled fluorophores (see Supplemental Figures S2 and S3). The beads were washed three times in 100 μ l PBS to remove any unreacted linker. In the second step, the glycosyl azides were covalently attached to the DBCO moieties displayed on the PS beads. The glycosyl azide solution was diluted to 0.5-1 mM in PBS by adding the respective volume of water and 10x PBS concentrate. Next, the DBCO-modified beads were resuspended in 20 μ l of glycosyl azide-containing buffer and incubated on a rotisserie overnight. Finally, the functionalized beads were washed three times in PBS and used the same day for the solid-state depletion assay.

2.4 Solid-state depletion or pull-down binding assay

The solid-state depletion assay follows the general steps used often to characterize CBM binding to insoluble substrates like microcrystalline or amorphous cellulose (43, 44). The working buffer (WB) used in the binding experiments was 10 mM PBS at pH 7.4 containing 0.2 mg/ml of bovine serum albumin (BSA) and Pluronic-F127, respectively. The CBMs were diluted in WB to a concentration between 50 and 1000 nM. First, the bead samples (20 μ l each) were resuspended in PCR tubes containing 100 μ l of WB and incubated on a rotisserie for 15 minutes to passivate the bead surface. After centrifugation (2000 x g for 1-3 minutes) and removal of the supernatant, the beads (cello-oligosaccharide-functionalized and non-specific binding control) were resuspended in 100 μ l of the prepared CBM dilutions and incubated on the rotisserie for 120 minutes at room temperature. Next, the beads were centrifuged and 90 μ l of supernatant was transferred to a new PCR tube, which was spun down again. Finally, 80 μ l of this supernatant was transferred to a black, clear bottom 96-well plate for unbound protein fluorescence quantitation. Two separate centrifugation steps were necessary to reduce the interference from beads being accidentally transferred to the 96-well plate.

The CBM concentration was determined by measuring the fluorescence signal of the appended GFP domain. The GFP-CBM standard curve was prepared from the same CBM dilutions used in the solid-state depletion assay and the fluorescence was quantified in a spectrophotometer (SpectraMax M5e, Molecular Devices) using 480 nm excitation, 512 nm emission, and a cut-off of 495 nm.

To obtain the free protein concentration, the readings of the non-specific binding samples at the same protein concentration were averaged. The bound protein concentration was determined by subtracting the free protein concentration from each cello-oligosaccharide-modified bead reading. Instead of using the mass of substrate added, the amount of bound protein was based on the number of theoretically available binding sites on the beads. Assuming a 100% conversion during both steps of the bead functionalization, this results in 5 nmol of total available binding sites per 20 µl of beads.

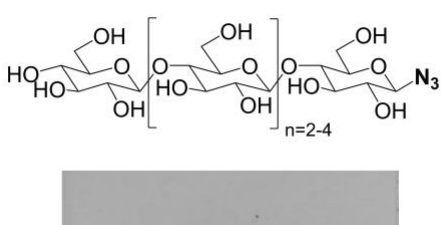
The Langmuir one-site binding model was used to determine the dissociation constant, K_d , and available binding sites on the cello-oligosaccharides functionalized bead surface,

 n_{max} . The model equation can be written as $B = \frac{n_{max}*F}{K_d + F}$, where B represents the concentration of bound protein and F the concentration of free/unbound protein. The model parameters were estimated using OriginPro 2020® using the built-in Levenberg-Marquardt algorithm.

3 Results

3.1 Azide modification of cello-oligosaccharides

The successful conversion of cello-oligosaccharides (i.e., cellotetraose, cellopentaose, and cellohexaose) to corresponding glycosyl azides was verified using TLC and representative results are shown in Figure 3. While there is only a small separation between the cello-oligosaccharides in the standard (Lane 1), the glycosyl azides separated well from the unmodified cello-oligosaccharides (Lanes 2-4, the red arrow indicates glycosyl azide). Using dialysis, it is not possible to separate the unmodified substrate from the product due to only a minor difference in molecular weight. However, dialysis efficiently removes the free azides, which would significantly interfere with the subsequent click reaction (see Supplemental Figure S4). Unmodified cello-oligosaccharides will be removed at washing steps after the click reaction, hence no separation between starting unreacted substrate and glycosyl azide was necessary.



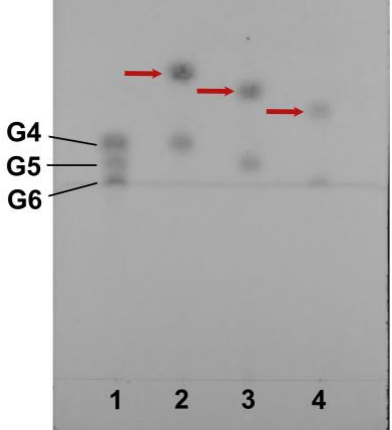


Figure 3: Thin-layer chromatography confirms the conversion of cello-oligosaccharides to azide-modified cello-oligosaccharides. The glycosyl azide products formed are indicated by the red arrow. The common structure of a glycosyl azide is shown on the top. Lane 1: Standard ladder of cellotetraose (G4), cellopentaose (G5), and cellohexaose (G6). Lane 2: Cellotetraose and cellotetraosyl azide (n=2). Lane 3: Cellopentaose and cellopentaosyl azide (n=3). Lane 4: Cellohexaose and cellohexaosyl azide (n=4).

The conversion was 84% for cellotetraose, while cellopentaose and cellohexaose showed a conversion of 59% and 63%, respectively. The total product yield from the reaction mixture after purification increased with the molecular weight of the carbohydrate and is 2, 6, and 9% for cellotetraose, cellopentaose, and cellohexaose respectively. The yield is significantly lower than previously reported (40), most likely due to sample loss during

dialysis instead of using High-Performance Liquid Chromatography (HPLC) as the purification method. Even though the membrane cutoff is less than 500 Da, most of the product is lost during the dialysis because it either diffuses through the pores and/or irreversibly binds to the cellulose ester membrane. Nevertheless, the removal of free azides using dialysis is a viable alternative in case HPLC at the preparative scale is not readily accessible.

3.2 Solid-state depletion protein-ligand binding assay

Image analysis of single beads revealed that CBMs bind specifically (p<0.05, n=50) to cello-oligosaccharide functionalized beads as shown in Supplemental Figure S5. The binding data and fitted Langmuir one-site binding model are summarized in Figure 4 and the region of less than 100nM of the binding isotherms is shown in Supplemental Figure S6. The dissociation constants and the maximum number of available binding sites are reported in Table 2. The p-values for each parameter estimation are summarized in Supplemental Table S2.

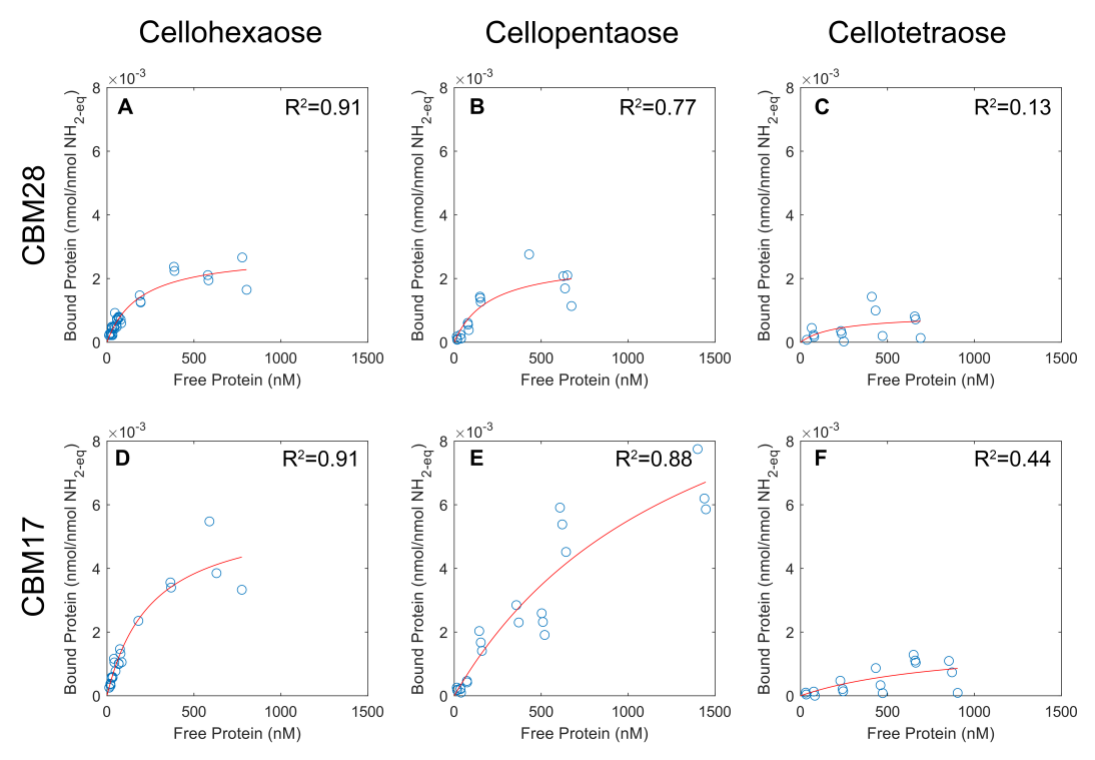


Figure 4: Binding data (blue circles) and fitted isotherms (red line) of CBM28 (top) and CBM17 (bottom) for cello-oligosaccharide-modified beads. The R^2 -value of the isotherm fit is shown in the top right corner of each panel. While the binding to cellohexaose-modified beads is similar for CBM17 and CBM28, there is a clear difference in binding for cellopentaose-modified beads. Both proteins show no significant (p>0.05) binding to cellotetraose-modified beads. Panel A-C) binding data for CBM28 on cellohexaose, cellopentaose, and cellotetraose-modified beads respectively. Panel D-F) binding data for CBM17 on cellohexaose, cellopentaose, and cellotetraose-modified beads respectively.

Both CBMs display a similar dissociation constant for cellohexaose-modified beads, however, the maximum number of binding sites is twice as high for CBM17. Differences in binding affinity become more evident when comparing the results for cellopentaose-modified beads. While the dissociation constant for CBM28 on cellopentaose-modified

beads is similar to cellohexaose-modified beads, CBM17 displays a \sim 5.5-fold increase in the dissociation constant and a \sim 2.3-fold increase in the number of binding sites. Although the CBM17 concentration was extended to 1.5 μ M, the binding curve of CBM17 on cellopentaose-modified beads did not fully level off as it was the case for CBM28. This, along with the increase in dissociation constants, indicates that CBM17 displays weaker binding towards cellopentaose-modified beads in our assay.

Table 2: Summary of Langmuir one site binding model fit parameters for CBM17 and CBM28 on cello-oligosaccharide-modified PS beads. The values indicate mean \pm SE. The unit of K_d is (nM), the unit of n_{max} is nmol protein/nmol NH_{2-eq}.

	Cellohexaose-beads		Cellopentaose-beads		Cellotetraose-beads	
	K_d	n_{max}	K_d	n_{max}	K_d	n_{max}
CBM28	189.3±28.5	0.28±1.9E-6	204.2±95.9	0.26±4.7E-6	217.0±378.3	0.09±5.6E-6
CBM17	256.9±61.3	0.58±6.1E-6	1404.3±615.5	1.32±35.5E-6	896.4±1515.5	0.17±17E-6

4 Discussion

We report the development of a solid-state depletion assay for testing protein binding to PS bead surface-immobilized glycans as an alternative method to characterize protein binding to soluble glycans. The modular approach using amino-modified surfaces will enable the adoption of the carbohydrate functionalization process to other analytical techniques such as QCM or SPR. The key step is the conversion of soluble glycans to glycosyl azides using Shoda's reagent, which can be adopted for various carbohydrates, such as xylo- or malto-oligosaccharides and even complex, branched sugars (40). In particular, the directed immobilization of complex carbohydrates as found in mammalian systems may be of great interest. Most of those glycans are immobilized on either antibodies or cell surfaces, which restrict their conformation and facilitate specific antibody-antigen interactions (45). Alternative chemical methods to site-specifically functionalize carbohydrates for immobilization on surfaces are time-consuming and often involve tedious protection/deprotection steps of hydroxy groups (46, 47), thus the use of Shoda's reagent is a promising and simple alternative. An excellent review on modifying unprotected carbohydrates is found elsewhere (38). Amino-modified beads are commercially available and QCM/SPR sensor surfaces made of guartz or borosilicate glass can be amino-functionalized with aminated silanes (48-50). The functionalization of amino-modified surfaces with DBCO moieties using amine-reactive hydroxysuccinimidyl (NHS) esters is straightforward and can easily be verified using azide-modified fluorophores as shown in Supplemental Figure S3. However, the removal of free azides from Shoda's reaction mixture is critical, as even a 0.1x molar excess of free unreacted azide can reduce click-chemistry reaction efficiency by more than 30% (see Supplemental Figure S4).

Previous MD simulations have revealed that the root-mean-square fluctuations or RMSF of cellopentaose upon binding to CBM17 and CBM28 can vary significantly depending on the ligand binding orientation (21). Based on those simulations, CBM17 seems to prefer binding from the reducing end while CBM28 prefers binding from the non-reducing end. The directed immobilization of cello-oligosaccharides in our bead assay displays the non-reducing end for binding. This could reduce protein access to favorable (more stable) ligand binding sites for CBM17, although the total number of available binding sites increased significantly compared to CBM28. In contrast, CBM28 prefers binding to

oligosaccharides from the non-reducing end based on available crystal structures, and as such only exhibits favorable binding interactions with the immobilized ligands. This difference in binding affinity between CBM17 and CBM28 was not previously detected using soluble substrates. In fact, the dissociation constant and number of binding sites for CBM28 are similar for cellohexaose- and cellopentaose-modified beads. Our preliminary findings suggest the possibility of a preferential binding orientation of cello-oligosaccharides by CBM families 17 and 28, which emphasize the need for in-depth exploration in future studies.

Both CBMs showed poor binding towards to cellotetraose-modified beads as seen in Figure 4, panels C and F and in the large error in the binding parameters data reported in Table 2 and p-values in Supplementary Table S2. This may be because the covalent linkage through the DBCO moiety could impose a steric hindrance on the reducing end of the cello-oligomer (see Figure 2). This steric hindrance effectively reduces the total number of pyranose rings available to engage via suitable hydrogen bonding and stacking interactions with the residues in the protein binding cleft. In other words, the cellohexaose-modified bead could be an effective cellopentaose-modified bead, and so on. This hypothesis may be supported by the fact that both CBM17 and CBM28 do not bind or just weakly bind to cello-oligosaccharides of a dp <4 (14, 16, 18). However, *A. akibai* CBM28 has a surface-exposed tryptophan at position 77 (see Figure 1), which may aid in binding cello-oligosaccharides in an alternative binding mode (12). In addition, CBM17 also lacks one aromatic residue in the binding pocket when compared to CBM28, which could explain the reduction in binding affinity as determined in our assay.

The dissociation constants as determined by our assay method were 40x-2200x lower compared to the results reported for the same proteins and substrates using ITC (11, 18). The main difference is that the substrate or ligand can freely diffuse in solution during ITC and is not immobilized to a solid surface. A reduction of the dissociation constant (or equivalent increase in binding affinity) has been previously reported for immobilized antibodies (51) towards respective antigen ligands. Further, the immobilization of carbohydrates on solid surfaces and presentation of smaller carbohydrates as multimeric ligands, enhances protein-carbohydrate interactions by orders of magnitudes (52–55). A similar phenomenon could explain the higher binding affinity seen for CBMs towards surface-immobilized oligosaccharides in our pull-down assay versus previously reported ITC assays using soluble ligands. It is likely that a reduction in the total degrees of freedom available for the surface-displayed ligands and well-defined ligand orientations could also result in tighter protein-ligand binding interactions at the solid-liquid interface. Similarly, type-B CBMs have been reported to show 10-to-100-fold higher binding affinity towards insoluble amorphous cellulose versus soluble cello-oligosaccharides (56). It was previously hypothesized that the high-affinity binding site interactions of CBMs with insoluble versus soluble ligands are due to relative gains in binding enthalpy (ΔH) and not gains seen in configurational entropy (ΔS). In contrast with results reported previously for CBM17/28 binding at high-affinity sites, the low-affinity binding interactions did show a gain in configurational entropy with a compensating enthalpic loss. However, since the structure of insoluble crystalline or amorphous cellulose is unknown, it has been challenging in the past to directly associate energetic observations made from ITC or pulldown binding assays with structural features of the ligand. Using well-defined

oligosaccharides immobilized to PS-beads, it would be now possible to systematically explore the binding interactions of proteins with surface-immobilized glycans.

The surface density of amino groups on the beads is approximately 1.7 NH₂/Å². Assuming that all amino groups are converted to DBCO groups for click-chemistry labeling to cellooligosaccharides and that one CBM covers around 50 Å², then around 165 cellooligosaccharides would be in close contact to one CBM. Our binding data suggests that less than 1% of the available NH₂ groups result in a successful CBM binding event. Steric hindrance from the PEG(4)-DBCO linker as well as incomplete reactions could significantly reduce the total number of cello-oligosaccharides close to each binding site. Nevertheless, it may be possible that *A. akibai* CBM28 may be able to engage with more than one cello-oligosaccharide at once due to W77, which is absent in CBM17 as well as *R. josui* CBM28. Future experiments could be carried out in which W77 is substituted to alanine or glycine and/or the binding site is further modified by replacing Y118 with alanine as well to only leave two aromatic residues in the binding pocket of CBM28. Nevertheless, our assay revealed a significant difference in dissociation constants if the substrate is displayed in an oriented manner. This could shed light on the reason for CBM17 and CBM28 to naturally occur in tandem.

Acknowledgments

S.P.S.C. acknowledges support from the NSF (CBET CAREER Award 1846797) and Rutgers SOE Startup Funds. Partial support was provided by NSF CBET Award 1704679.

References

- 1. M. E. Himmel, *et al.*, Biomass recalcitrance: Engineering plants and enzymes for biofuels production. *Science* (80-.). **315**, 804–807 (2007).
- 2. S. P. S. Chundawat, G. T. Beckham, M. E. Himmel, B. E. Dale, Deconstruction of Lignocellulosic Biomass to Fuels and Chemicals. *Annu. Rev. Chem. Biomol. Eng.* **2**, 121–145 (2011).
- 3. C. M. Payne, et al., Fungal cellulases. Chem. Rev. 115, 1308–1448 (2015).
- 4. M. Linder, T. T. Teeri, The roles and function of cellulose-binding domains. *J. Biotechnol.* **57**, 15–28 (1997).
- 5. O. Shoseyov, Z. Shani, I. Levy, Carbohydrate Binding Modules: Biochemical Properties and Novel Applications. *Microbiol. Mol. Biol. Rev.* **70**, 283–295 (2006).
- 6. A. B. Boraston, D. N. Bolam, H. J. Gilbert, G. J. Davies, Carbohydrate-binding modules: fine-tuning polysaccharide recognition. *Biochem. J.* **382**, 769–781 (2004).
- 7. A. B. Boraston, *et al.*, Differential oligosaccharide recognition by evolutionarily-related β-1,4 and β-1,3 glucan-binding modules. *J. Mol. Biol.* **319**, 1143–1156 (2002).
- 8. L. Von Schantz, *et al.*, Structural basis for carbohydrate-binding specificity-A comparative assessment of two engineered carbohydrate-binding modules. *Glycobiology* **22**, 948–961 (2012).
- 9. E. Brun, *et al.*, Structure and binding specificity of the second N-terminal cellulose-binding domain from Cellulomonas fimi endoglucanase C. *Biochemistry* **39**, 2445–2458 (2000).
- 10. M. Alahuhta, *et al.*, The unique binding mode of cellulosomal CBM4 from clostridium thermocellum cellobiohydrolase A. *J. Mol. Biol.* **402**, 374–387 (2010).
- 11. V. Notenboom, *et al.*, Recognition of cello-oligosaccharides by a family 17 carbohydrate-binding module: An X-ray crystallographic, thermodynamic and mutagenic study. *J. Mol. Biol.* **314**, 797–806 (2001).
- 12. S. Jamal, D. Nurizzo, A. B. Boraston, G. J. Davies, X-ray crystal structure of a non-crystalline cellulose-specific carbohydrate-binding module: CBM28. *J. Mol. Biol.* **339**, 253–258 (2004).
- 13. K. Tsukimoto, *et al.*, Recognition of cellooligosaccharides by a family 28 carbohydrate-binding module. *FEBS Lett.* **584**, 1205–1211 (2010).
- 14. Y. Araki, S. Karita, A. Tanaka, M. Kondo, M. Goto, Characterization of family 17 and family 28 carbohydrate-binding modules from clostridium josui Cel5A. *Biosci. Biotechnol. Biochem.* **73**, 1028–1032 (2009).
- 15. A. B. Boraston, E. Kwan, P. Chiu, R. A. J. Warren, D. G. Kilburn, Recognition and hydrolysis of noncrystalline cellulose. *J. Biol. Chem.* **278**, 6120–6127 (2003).
- 16. A. B. Boraston, P. Chiu, R. A. J. Warren, D. G. Kilburn, Specificity and affinity of substrate binding by a family 17 carbohydrate-binding module from Clostridium cellulovorans cellulase 5A. *Biochemistry* **39**, 11129–11136 (2000).
- 17. T. Liu, *et al.*, Binding affinity of family 4 carbohydrate binding module on cellulose films of nanocrystals and nanofibrils. *Carbohydr. Polym.* **251**, 116725 (2021).

- 18. A. B. Boraston, M. Ghaffari, R. A. J. Warren, D. G. Kilburn, Identification and glucan-binding properties of a new carbohydrate-binding module family. *Biochem. J.* **361**, 35 (2002).
- 19. P. Tomme, A. L. Creagh, D. G. Kilburn, C. A. Haynes, Interaction of polysaccharides with the N-terminal cellulose-binding domain of Cellulomonas fimi CenC. 1. Binding specificity and calorimetric analysis. *Biochemistry* **35**, 13885–13894 (1996).
- 20. S. J. Charnock, *et al.*, Promiscuity in ligand-binding: The three-dimensional structure of a Piromyces carbohydrate-binding module, CBM29-2, in complex with cello-and mannohexaose. *Proc. Natl. Acad. Sci. U. S. A.* **99**, 14077–14082 (2002).
- 21. A. A. Kognole, C. M. Payne, Cellulose-specific Type B carbohydrate binding modules: Understanding oligomeric and non-crystalline substrate recognition mechanisms. *Biotechnol. Biofuels* **11**, 1–16 (2018).
- 22. A. A. Kognole, C. M. Payne, Cello-oligomer-binding dynamics and directionality in family 4 carbohydrate-binding modules. *Glycobiology* **25**, 1100–1111 (2015).
- 23. J. B. Coutinho, B. Moser, D. G. Kilburn, R. A. J. Warren, R. C. Miller, Nucleotide sequence of the endoglucanase C gene (cenC) of Cellulomonas fimi, its high-level expression in Escherichia coli, and characterization of its products. *Mol. Microbiol.* **5**, 1221–1233 (1991).
- 24. D. E. Ciolacu, F. Ciolacu, V. I. Popa, Amorphous cellulose structure and characterization. *Cellul. Chem. Technol.* **45**, 13–21 (2011).
- 25. B. W. McLean, *et al.*, Carbohydrate-binding modules recognize fine substructures of cellulose. *J. Biol. Chem.* **277**, 50245–50254 (2002).
- 26. A. W. Blake, *et al.*, Understanding the biological rationale for the diversity of cellulose-directed carbohydrate-binding modules in prokaryotic enzymes. *J. Biol. Chem.* **281**, 29321–29329 (2006).
- 27. Y. Araki, S. Karita, T. Tsuchiya, M. Kondo, M. Goto, Family 17 and 28 carbohydrate-binding modules discriminated different cell-wall sites in sweet potato roots. *Biosci. Biotechnol. Biochem.* **74**, 802–805 (2010).
- 28. M. Marradi, M. Martín-Lomas, S. Penadés, *Glyconanoparticles. Polyvalent Tools to Study Carbohydrate-Based Interactions* (2010).
- 29. B. Kang, T. Opatz, K. Landfester, F. R. Wurm, Carbohydrate nanocarriers in biomedical applications: Functionalization and construction. *Chem. Soc. Rev.* **44**, 8301–8325 (2015).
- 30. N. M. B. Smeets, S. Imbrogno, S. Bloembergen, Carbohydrate functionalized hybrid latex particles. *Carbohydr. Polym.* **173**, 233–252 (2017).
- 31. K. Sangseethong, "Immobilized cellooligosaccharides in the study of trichoderma reesei cellobiohydrolases." (1999).
- 32. H. Hasuda, O. H. Kwon, I. K. Kang, Y. Ito, Synthesis of photoreactive pullulan for surface modification. *Biomaterials* **26**, 2401–2406 (2005).
- 33. H. J. Lee, *et al.*, Preparation of photoreactive azidophenyl hyaluronic acid derivative: Protein immobilization for medical applications. *Macromol. Res.* **21**, 216–220 (2013).
- 34. X. Wang, E. Matei, A. M. Gronenborn, O. Ramström, M. Yan, Direct measurement of

- glyconanoparticles and lectin interactions by isothermal titration calorimetry. *Anal. Chem.* **84**, 4248–4252 (2012).
- 35. C. C. Lin, *et al.*, Quantitative analysis of multivalent interactions of carbohydrate-encapsulated gold nanoparticles with concanavalin A. *Chem. Commun.* **3**, 2920–2921 (2003).
- 36. E. Mahon, T. Aastrup, M. Barboiu, Multivalent recognition of lectins by glyconanoparticle systems. *Chem. Commun.* **46**, 5491–5493 (2010).
- 37. A. J. Fairbanks, Applications of Shoda's reagent (DMC) and analogues for activation of the anomeric centre of unprotected carbohydrates. *Carbohydr. Res.* **499**, 108197 (2021).
- 38. K. Villadsen, M. C. Martos-Maldonado, K. J. Jensen, M. B. Thygesen, Chemoselective Reactions for the Synthesis of Glycoconjugates from Unprotected Carbohydrates. *ChemBioChem* **18**, 574–612 (2017).
- 39. S. P. S. Chundawat, *et al.*, Molecular origins of reduced activity and binding commitment of processive cellulases and associated carbohydrate-binding proteins to cellulose III. *J. Biol. Chem.* **296**, 100431 (2021).
- 40. T. Tanaka, H. Nagai, M. Noguchi, A. Kobayashi, S. I. Shoda, One-step conversion of unprotected sugars to β-glycosyl azides using 2-chloroimidazolinium salt in aqueous solution. *Chem. Commun.*, 3378–3379 (2009).
- 41. O. Kosik, J. R. Bromley, M. Busse-Wicher, Z. Zhang, P. Dupree, *Studies of enzymatic cleavage of cellulose using polysaccharide analysis by carbohydrate gel electrophoresis (PACE)*, 1st Ed. (Elsevier Inc., 2012).
- 42. A. Angelov, *et al.*, A metagenome-derived thermostable β-glucanase with an unusual module architecture which defines the new glycoside hydrolase family GH148. *Sci. Rep.* **7**, 1–13 (2017).
- 43. D. W. Abbott, A. B. Boraston, *Quantitative approaches to the analysis of carbohydrate-binding module function*, 1st Ed. (Elsevier Inc., 2012).
- 44. B. Nemmaru, *et al.*, Reduced type-A carbohydrate-binding module interactions to cellulose I leads to improved endocellulase activity. *Biotechnol. Bioeng.* **118**, 1141–1151 (2021).
- 45. S. Defaus, P. Gupta, D. Andreu, R. Gutierrez-Gallego, Mammalian protein glycosylation structure versus function. *Analyst* **139**, 2944–2967 (2014).
- 46. K. Sangseethong, M. H. Penner, p-Aminophenyl β-cellobioside as an affinity ligand for exo-type cellulases. *Carbohydr. Res.* **314**, 245–250 (1998).
- 47. O. Akpinar, "Preparation and modification of cellooligosaccharides." (2002).
- 48. M. Zhu, M. Z. Lerum, W. Chen, How to prepare reproducible, homogeneous, and hydrolytically stable aminosilane-derived layers on silica. *Langmuir* **28**, 416–423 (2012).
- 49. R. G. Acres, *et al.*, Molecular structure of 3-aminopropyltriethoxysilane layers formed on silanol-terminated silicon surfaces. *J. Phys. Chem. C* **116**, 6289–6297 (2012).
- 50. J. Kim, P. Seidler, L. S. Wan, C. Fill, Formation, structure, and reactivity of aminoterminated organic films on silicon substrates. *J. Colloid Interface Sci.* **329**, 114–119 (2009).

- 51. N. Tajima, M. Takai, K. Ishihara, Significance of antibody orientation unraveled: Well-oriented antibodies recorded high binding affinity. *Anal. Chem.* **83**, 1969–1976 (2011).
- 52. X. L. Sun, W. Cui, C. Haller, E. L. Chaikof, Site-specific multivalent carbohydrate labeling of quantum dots and magnetic beads. *ChemBioChem* **5**, 1593–1596 (2004).
- 53. R. Liang, *et al.*, Polyvalent binding to carbohydrates immobilized on an insoluble resin. *Proc. Natl. Acad. Sci. U. S. A.* **94**, 10554–10559 (1997).
- 54. P. Adler, *et al.*, High affinity binding of the Entamoeba histolytica lectin to polyvalent nacetylgalactosaminides. *J. Biol. Chem.* **270**, 5164–5171 (1995).
- 55. M. Reynolds, M. Marradi, A. Imberty, S. Penadés, S. Pérez, Influence of ligand presentation density on the molecular recognition of mannose-functionalised glyconanoparticles by bacterial lectin BC2L-A. *Glycoconj. J.* **30**, 747–757 (2013).
- 56. A. B. Boraston, The interaction of carbohydrate-binding modules with insoluble non-crystalline cellulose is enthalpically driven. *Biochem. J.* **385**, 479–484 (2005).

Supplementary Information (SI) for

Oriented Display of Cello-Oligosaccharides for Pull-down Binding Assays to Distinguish Binding Preferences of Glycan Binding Proteins

Markus Hackla, Zachary Powera, Shishir P. S. Chundawata,*

^a Department of Chemical and Biochemical Engineering, Rutgers, The State University of New Jersey, Piscataway NJ, 08854

*Corresponding author: Shishir P. S. Chundawat (ORCID: 0000-0003-3677-6735). Department of Chemical & Biochemical Engineering, Rutgers, The State University of New Jersey, 98 Brett Road Piscataway, NJ 08854. Phone: +1-848-445-3678

Email: shishir.chundawat@rutgers.edu

This PDF file includes:

Supplementary text Supplementary Figures S1 to S6 Supplementary Tables S1 to S2 SI References

Gene sequences for CBM17 and CBM28

As shown in Supplemental Figure S1, both CBMs were fused to His₈-GFP separated by a flexible linker domain as previously described (1). The gene sequences for linker and CBM can be found in Supplemental Table S1.

Single polystyrene (PS) bead analysis using wide-field fluorescence microscopy

To verify the proposed reactions and binding events, a method to analyze single PS beads using fluorescence microscopy was developed. Fluorescence images were taken at 20x magnification with a scientific camera (Kiralux, Thorlabs Inc.) using µManager (2) on an inverted fluorescence microscope (Olympus IX 71) equipped with the necessary filters to monitor green fluorescence. The individual steps in image processing and analysis were carried out in Fiji (3) and are shown in Supplemental Figure S2. Each image was first corrected for background and shading (4), followed by thresholding to remove the background. The exact values for thresholding depend on the signal/noise ratio of the particular experiment and were set such that the outline of single beads was clearly visible. Finally, 50 single beads were randomly chosen that were not in close proximity to other beads and the mean value was recorded.

Confirmation of DBCO linker functionalization of aminated PS beads

The functionalization of aminated beads with the NHS-PEG(4)-DBCO linker was confirmed by using an azide labeled fluorophore (N_3 -488, or Rhodamine 110-azide) which reacts with the DBCO moiety on the beads. A schematic overview of the experiment is shown in Supplemental Figure S3-A. Image analysis was carried out for single beads as described above. It is important that all buffers are free of amines or azides as that would interfere with the functionalization steps. First, 20 μ I of aminated beads were washed three times in 100 μ I PBS pH 7.4 and equally split into two PCR tubes. Next, one sample of beads was resuspended in 10 μ I PBS containing 250 μ M NHS-PEG(4)-DBCO, whereas the other one was resuspended in PBS only. The beads were incubated on a rotisserie overnight at room temperature, followed by three washes of 100 μ I PBS each. Next, both samples were resuspended in 10 μ I PBS containing 10 μ M of N_3 -488 and incubated on a rotisserie for 120 minutes. Finally, both samples were washed three times with 100 μ I PBS and imaged on the fluorescence microscope. As it can be seen in Supplemental Figure S3-B, the addition of the NHS-PEG(4)-DBCO linker results in a significantly higher average pixel intensity compared to the control, thus verifying that the beads were successfully functionalized with DBCO moieties for subsequent click reactions.

Influence of free azides on click reaction of DBCO-functionalized beads

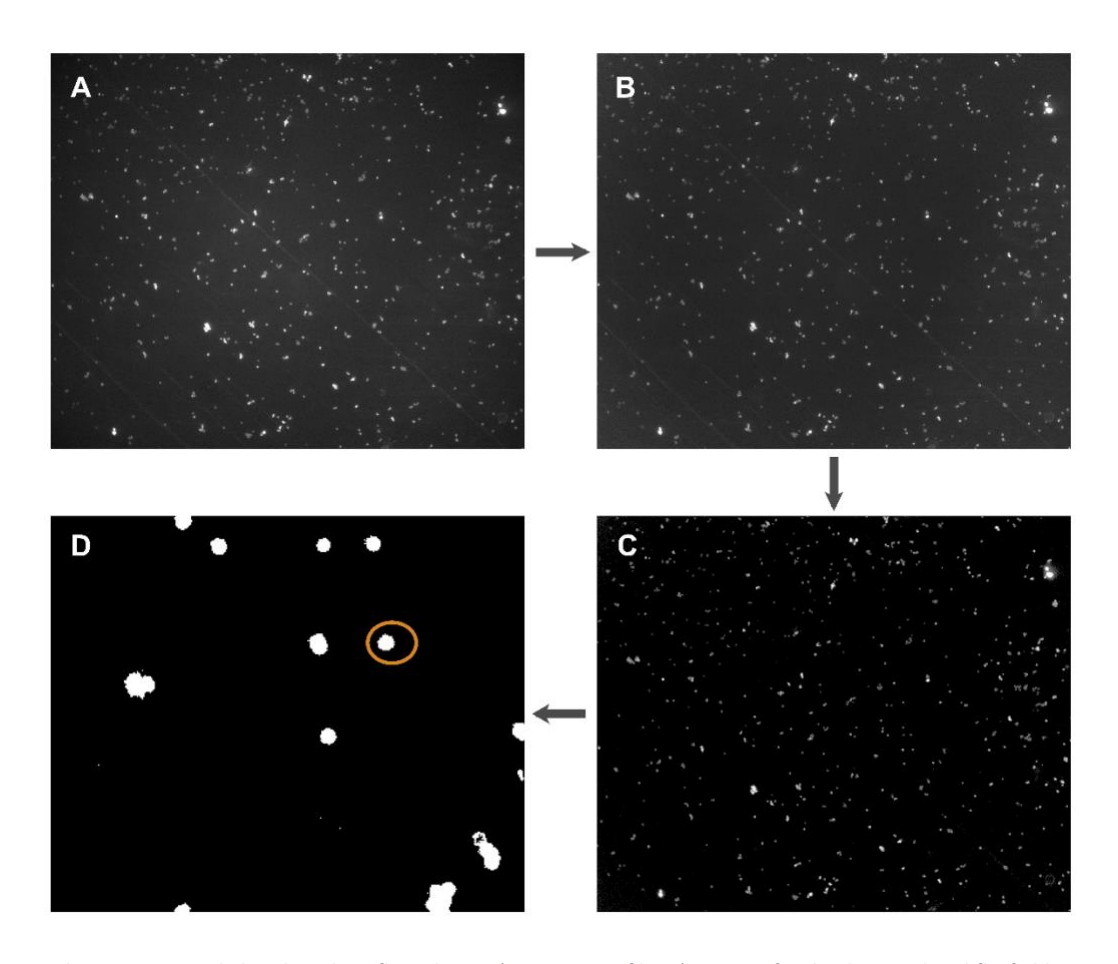
The conversion of carbohydrates to glycosyl azides requires the presence of 50-120x molar excess of sodium azide. The removal of those free azides from the reaction mixture is important since the free azides compete with the click reaction of glycosyl azides. To assess the influence of free azides on the click reaction, the N_3 -488 reaction described above was carried out in the presence of varying amounts of sodium azide. The functionalization of beads with DBCO and all washing steps and analysis were identically carried out as described above. The only difference was that N_3 -488 was diluted to 10 μ M in PBS containing 100x, 10x, 1x, 0.1x, and 0x molar excess of sodium azide with respect to N_3 -488. As shown in Supplemental Figure S4, even a 0.1x molar excess of free sodium azide can significantly reduce the obtained fluorescence signal. The images were taken at 300 ms exposure time and no fluorescence signal was detected for the 100x sample at this setting.

Binding specificity of green fluorescent protein (GFP)-CBM28 to cello-oligosaccharide functionalized beads

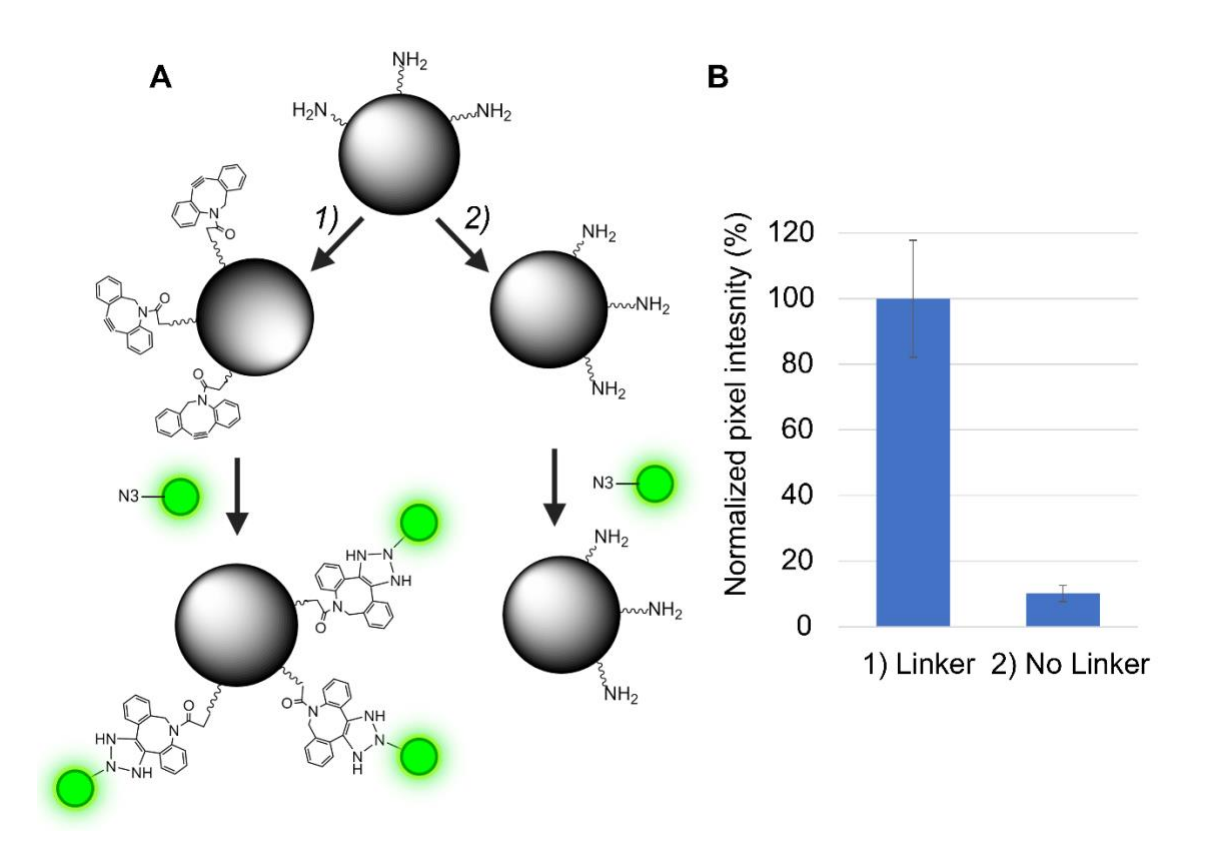
Bead samples were functionalized with DBCO as described above. Instead of using N_3 -488, the bead samples were resuspended in 10 μ l PBS containing either 250 μ M cellopentaosyl azide, 250 μ M cellopentaose, or only PBS and allowed to mix on a rotisserie over-night at room temperature. Next, the beads were washed three times in 100 μ l PBS and resuspended in 100 μ l working buffer (WB, PBS containing 0.2 mg/ml of BSA and Pluronic-F127) to passivate the surface for 15 minutes. Following passivation, the beads were spun down and resuspended in 10 μ l WB containing 1 μ M of GFP-CBM28 and incubated for two hours at room temperature on a rotisserie. Finally, the beads were washed twice with 100 μ l WB, resuspended in 10 μ l WB and the samples were imaged and analyzed as described above. Supplemental Figure S5 summarizes the normalized mean pixel intensity from multiple beads. The obtained fluorescence from a bead sample functionalized with cellopentaosyl azide is significantly (p<0.05, n=50) higher compared to the controls. Furthermore, the difference between the bead sample exposed to unmodified cellopentaose and only PBS is insignificant (p>0.05, n=50). These results indicate a successful functionalization of beads with azido-labeled carbohydrates and the ability of type B CBMs to bind to the click-chemistry immobilized carbohydrates displayed on PS beads.



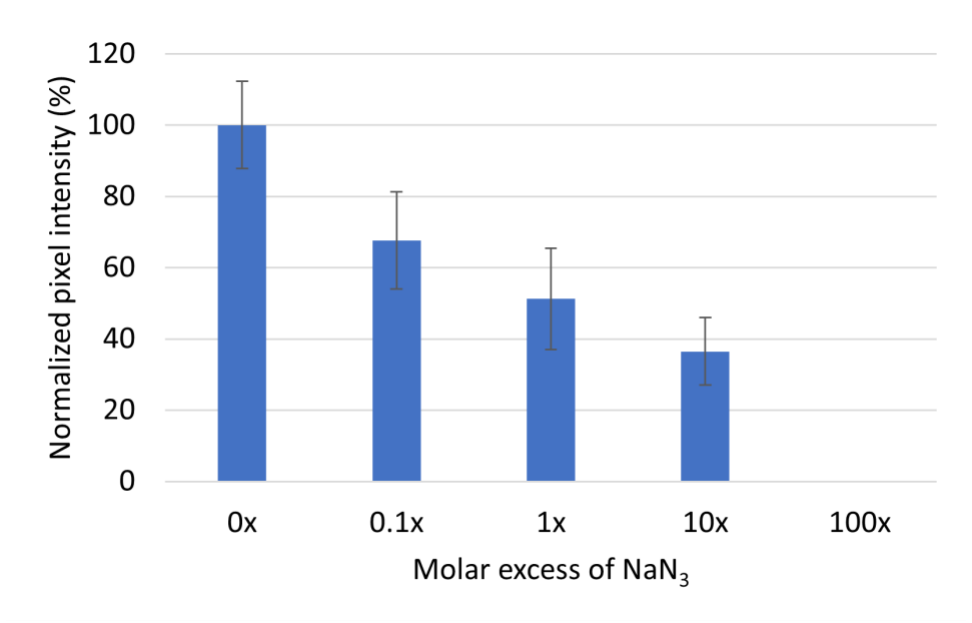
Supplemental Figure S1: Domain overview of CBM fusion constructs. Both CBMs are fused to His_8 -GFP via a flexible linker region. The individual sequences are found in Supplementary Table S1.



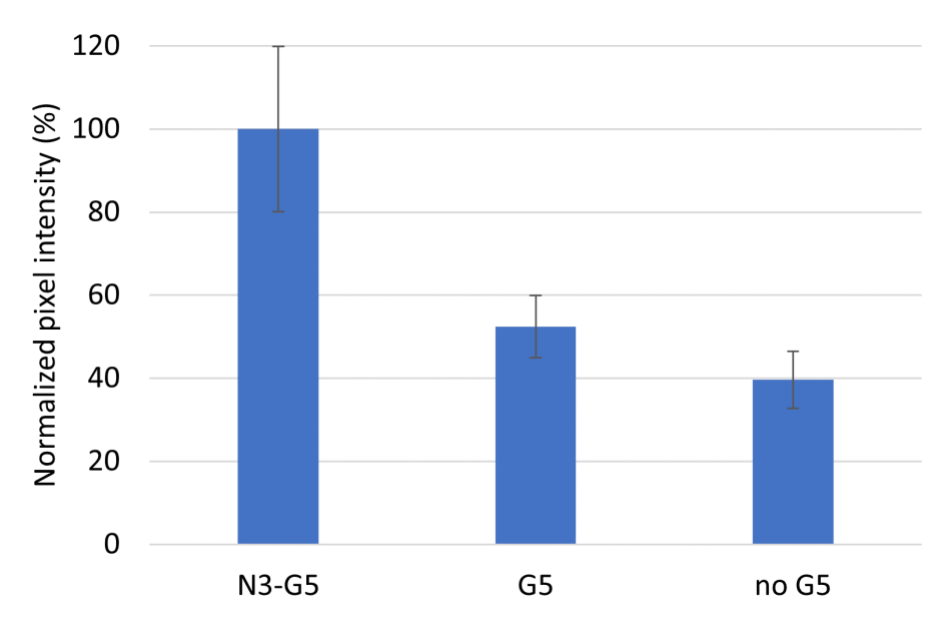
Supplemental Figure S2: Single bead analysis flow chart. A) Raw image file. B) Image after background and flatfield correction. C) Image after thresholding and background removal. D) Only single, isolated beads such as the one circled in orange are analyzed.



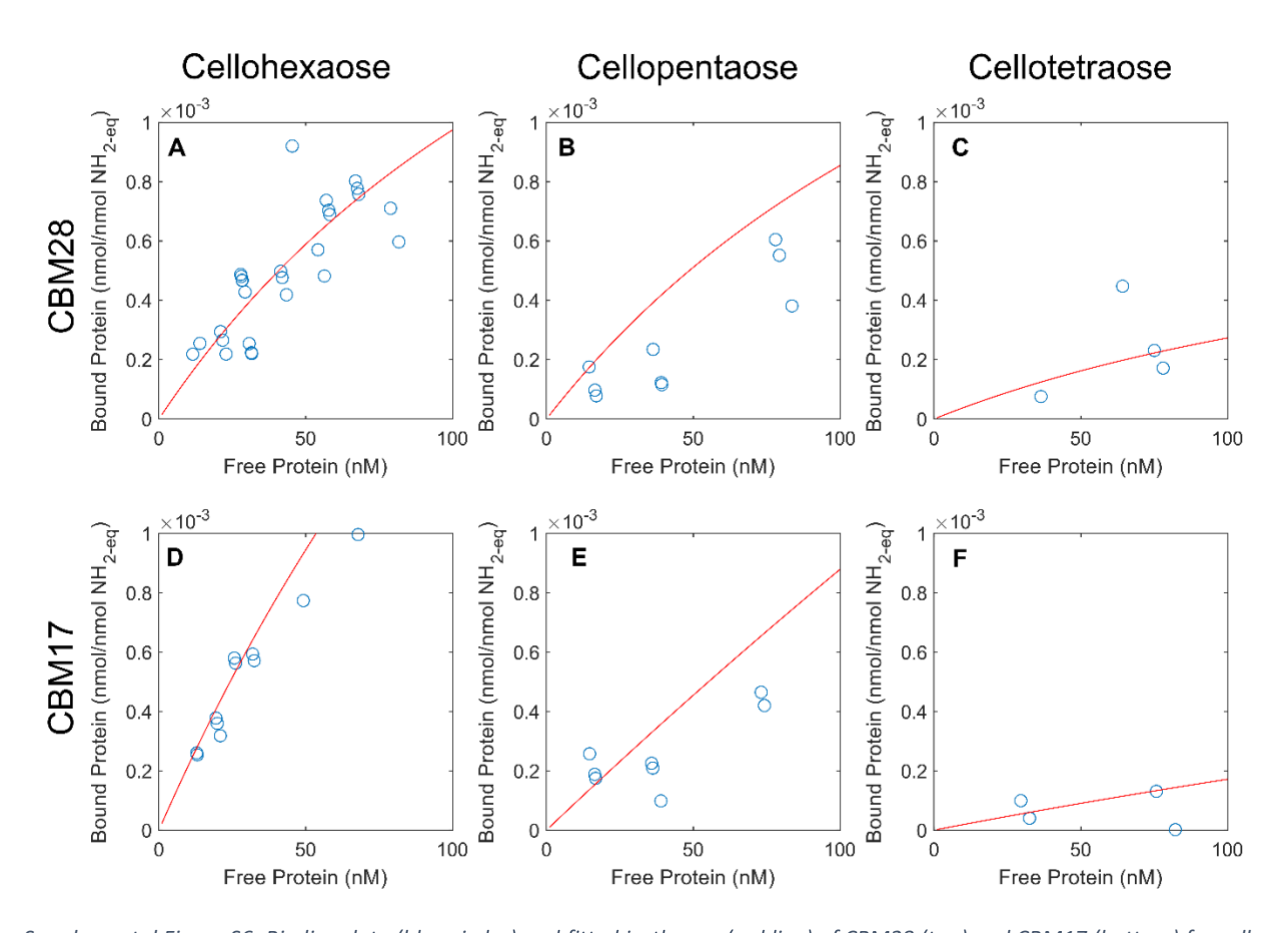
Supplemental Figure S3: Verification of DBCO functionalization of aminated PS beads. A) Schematic overview of the experiment where in route 1) beads are functionalized with NHS-PEG(4)-DBCO and in route 2) beads are just incubated in PBS. B) Results of single bead fluorescence analysis. The fluorescence intensity is significantly (p<0.05, n=50) higher for DBCO functionalized beads. The pixel intensity is normalized to the intensity value of the linker-containing sample. Error bars represent the standard deviation of 50 analyzed beads.



Supplemental Figure S4: Influence of free azides on the click reaction between DBCO-modified beads and N_3 -488. Even a small molar excess of free azides significantly (p<0.05, n=50) reduces the fluorescence signal, indicating a strong interference of free azides. The pixel intensity is normalized to the intensity value of the 0x molar excess sample. No fluorescence signal for the 100x sample was detected at the 300 ms exposure time. Error bars represent the standard deviation of 50 analyzed beads.



Supplemental Figure S5: Type-B CBMs specifically bind to PS beads covalently functionalized with oligosaccharides. The obtained fluorescence intensity of carbohydrate modified beads is significantly (p<0.05, n=50) higher compared to the control experiments with unmodified cellopentaose or in the absence of any carbohydrate. The pixel intensity is normalized to the intensity value of the N3-G5 sample. Error bars represent the standard deviation of 50 analyzed beads.



Supplemental Figure S6: Binding data (blue circles) and fitted isotherms (red line) of CBM28 (top) and CBM17 (bottom) for cellooligosaccharide-modified beads in the range 0-100 nM. Panel A-C) binding data for CBM28 on cellohexaose, cellopentaose and cellotetraose-modified beads respectively. Panel D-F) binding data for CBM17 on cellohexaose, cellopentaose and cellotetraosemodified beads respectively.

Supplemental Table S1: DNA sequences of linker domain, CBM17, and CBM28.

Domain	DNA sequence	Organism Source
His-8	ATGGGACATCACCATCACCATCACCATGCATCCGAAAACCT GTACTTCCAGGCGATCGCC	N/A
GFP	TCCAAAGGTGAAGAACTGTTCACCGGTGTTGTTCCGATCCTGG TTGAACTGGACGGTGACGTTAACGGTCACAAATTCTCCGTTTCC GGTGAAGGTGAAGGTGACGCTACCTACGGTAAACTGACCCTGA AATTCATCTGCACCACCGGTAAACTGCCGGTTCCGTGGCCGAC CCTGGTTACCACCCTGACCTACGGTGTTCAGTGCTTCTCCCGT TACCCGGACCACATGAAACAGCACGACTTCTTCAAATCCGCTAT GCCGGAAGGTTACGTTCAGGAACGTACCATCTCCTTCAAAGAC GACGGTAACTACAAAACCCGTGCTGAAGTTAAATTCGAAGGTG ACACCCTGGTTAACCGTATCGAACTGAAAGGTATCGACTTCAAA GAAGACGGTAACATCCTGGGTCACAAACTGGAATACAACTACA ACTCCCACAACGTTTACATCACCGCTGACAAACAGAAAAACGGT ATCAAAGCTAACTTCAAAATCCGTCACAACATCGAAGACGGTTC CGTTCAGCTGGCTGACCACTACCAGCAGAACACCCCGATCGGT GACGGTCCGGTTCTGCTGCCGGACAACACCACTACCTGTCCACCC AGTCCGCTCTGTCCAAAGACCCGAACAAAACGTGACCACAT GGTTCTGCTGGAATTCGTTACCGCTGCTGGTATCACCCACGGT ATGGACGAACTGTACAAA	Aequorea victoria
Linker	GGTTTAAACGCGACTCCCACTAAAGGTGCCACTCCTACCAATA CGGCGACTCCGACTAAGTCGGCAACGGCAACGCCCACTCGCC CCAGCGTACCGACCAATACTCCGACTAATACCCCGGCGAACAC CCTTAAG	N/A
CBM17	AGCCAACCGACCGCCCGAAAGATTTTTCCTCAGGTTTCTGGG ACTTTAACGATGGCACGACCCAGGGTTTCGGCGTGAATCCGGA CTCGCCGATTACGGCAATCAACGTTGAAAATGCTAACAATGCG CTGAAAATTAGCAACCTGAACAGCAAAGGTAGTAACGATCTGTC CGAAGGCAATTTTTGGGCCAACGTCCGCATCTCAGCAGACATT TGGGGTCAATCGATCAATATTTATGGCGATACCAAACTGACGAT GGACGTGATCGCTCCGACCCCGGTTAACGTCAGCATTGCGGC CATCCCGCAGTCTAGTACGCATGGTTGGGGCAATCCGACCCGT GCAATTCGCGTGTGGACGAACAATTTCGTTGCTCAAACCGATG GTACGTATAAAGCGACCCTGACGATCTCCACCAACGACTCACC GAATTTTAACACCATTGCCACCGATGCAGCCGACTCGGTCGTT ACCAATATGATCCTGTTCGTGGGCTCCAACAGCGATAATATTAG CCTGGACAACATCAAATTTACCAAA	Clostridium cellulovarans
CBM28	ACCCAGAGCGCACCGAAGTGGAAATTCCGGTGGTGCATGAT CCGAAAGGCGAAGCGGTGCTGCCGAGCGTGTTTGAAGATGGC ACCCGTCAGGGCTGGGATTGGGCGGCGCAAAGCGGCGTGAAA ACCGCGCTGACCATTGAAGAAGCGAACGGCAGCAACGCGCTG AGCTGGGAATTTGGCTATCCGGAAGTGAAACCGAGCGATAACT GGGCGACCGCGCGCGTCTGGATTTTTGGAAAAGCGATCTGG TGCGTGGCGAAAACGATTATGTGACCTTTGATTTTTACCTGGAC CCAGTGCGTGCGACCGAAGGCGCGATGAACATTAACCTGGTGT TTCAGCCGCCGACCAACGGCTATTGGGTGCAGGCGCCGAAAA CCTATACCATTAACTTTGATGAACTGGAAGAACCGAACC	Alkalihalobacillus akibai (Bacillus sp. 1139)

Supplemental Table S2: p-values for fit parameters corresponding to main text Table 2. The p-values for cellotetraose are > 0.05 indicating a weak fit of the model.

	Cellohexaose-beads		Cellopentaose-beads		Cellotetraose-beads	
	K_d	n_{max}	K_d	n_{max}	K_d	n_{max}
CBM28	1.29E-07	1.33E-16	0.05027	6.18E-05	0.57787	0.14801
CBM17	4.11E-04	4.69E-09	0.0336	0.00134	0.56302	0.33078

SI references

- 1. S. P. S. Chundawat, *et al.*, Molecular origins of reduced activity and binding commitment of processive cellulases and associated carbohydrate-binding proteins to cellulose III. *J. Biol. Chem.* **296**, 100431 (2021).
- 2. A. Edelstein, N. Amodaj, K. Hoover, R. Vale, N. Stuurman, Computer Control of Microscopes Using µManager. *Curr. Protoc. Mol. Biol.* **92**, 1–17 (2010).
- 3. J. Schindelin, *et al.*, Fiji: An open-source platform for biological-image analysis. *Nat. Methods* **9**, 676–682 (2012).
- 4. M. A. Model, J. K. Burkhardt, A standard for calibration and shading correction of a fluorescence microscope. *Commun. Clin. Cytom.* **46**, 309–316 (2001).